

# Heterogeneous Acceleration Pipeline for Recommendation System Training

Muhammad Adnan\*    Yassaman Ebrahimzadeh Maboud\*    Divya Mahajan<sup>+</sup>    Prashant J. Nair\*  
The University of British Columbia\*    Microsoft<sup>+</sup>  
{adnan,yassaman,prashantnair}@ece.ubc.ca    divya.mahajan@microsoft.com

## Abstract

Recommendation systems are unique as they show a conflation of compute and memory intensity due to their deep learning and massive embedding tables. Training these models typically involve a hybrid CPU-GPU mode, where GPUs accelerate the deep learning portion and the CPUs store and process the memory-intensive embedding tables. The hybrid mode incurs a substantial CPU-to-GPU transfer time and relies on main memory bandwidth to feed embeddings to GPU for deep learning acceleration. Alternatively, we can store the entire embeddings across GPUs to avoid the transfer time and utilize the GPU’s High Bandwidth Memory (HBM). This approach requires GPU-to-GPU backend communication and scales the number of GPUs with the size of the embedding tables. To overcome these concerns, this paper offers a heterogeneous acceleration pipeline, called Hotline.

Hotline leverages the insight that only a small number of embedding entries are accessed frequently, and can easily fit in a single GPU’s HBM. Hotline implements a data-aware and model-aware scheduling pipeline that utilizes the (1) CPU main memory for not-frequently-accessed embeddings and (2) GPUs’ local memory for frequently-accessed embeddings. Hotline improves the training throughput by dynamically stitching the execution of popular and not-popular inputs through a novel hardware accelerator and feeding to the GPUs. Results on real-world datasets and recommender models show that Hotline reduces the average training time by 3× and 1.8× in comparison to Intel-optimized CPU-GPU DLRM and HugeCTR-optimized GPU-only baseline, respectively. Hotline increases the overall training throughput to 35.7 epochs/hour in comparison to 5.3 epochs/hour for the Intel-optimized DLRM baseline.

## 1. Introduction

Recommendation models are increasingly becoming one of the deployed Machine Learning (ML) workload. Meta reports that 50% of their training cycles are devoted to training deep learning based recommendation models [6]. Recommender models are a disaggregated conflation of compute-intensive neural networks and memory-intensive embedding tables [21]. The embedding tables store the user and item features. The size of the embedding tables is expected to increase as more users and items interact. For instance, a recent work from Baidu [57] shows that production-scale recommendation models are reaching 10 TBs in size.

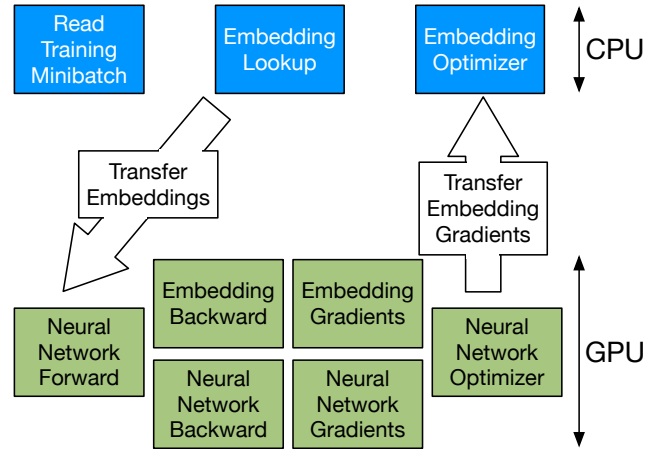


Figure 1: The execution flow of a typical recommendation model in the hybrid CPU-GPU mode. Due to their large sizes, the embedding tables are stored and processed on CPUs. The GPUs process the neural layers.

Deep Learning (DLRM) [40] and Time-Based Sequence (TBSM) [23] Models are often trained in a hybrid setup of CPUs and GPUs. Figure 1 shows the training flow of a recommender model in the hybrid mode with the CPU handling the embedding data by offering its high memory capacity. The GPUs offer high compute throughput and perform data parallel execution of the DNN phase [26]. A training iteration includes reading the inputs, fetching corresponding embedding data, neural network and embedding computations, and any data transfer required to update the model.

The hybrid execution has low efficiency as (1) GPUs rely on the CPU to provide all the embeddings to execute the DNN; (2) the low-bandwidth main memory acts as a bottleneck during embedding-bag operation and embedding-weights’ optimization; and (3) it does not fully utilize the GPU for the entirety of the training process – as the embeddings are executed on the CPU. Alternatively, one can also use multiple GPUs to store a single-copy of the embeddings and train in a model-parallel fashion. For instance, HugeCTR [2] uses GPU memories to store the embeddings. Such techniques require the number of GPUs to scale with the embedding size while the GPUs remain under-utilized by the neural portion.

Instead in this work we offer a novel *throughput-optimized* heterogeneous acceleration pipeline called Hotline. Hotline aims to efficiently use the system resources - memory and compute - to pipeline the end-to-end training of large-scale

recommender models. *Hotline* is the first work to enable the GPU-only execution of the entire training of the recommender model, i.e., forward pass, backward pass, loss function, and optimizer for both embeddings and DNN portion, without requiring to store the entirety of embeddings on GPUs. As *Hotline* does not require each GPU to act as a bank for all embeddings the number of GPU devices does not scale with the model size. The pipeline also mitigates the inefficiencies of the CPU-GPU hybrid execution mode by hiding the latency of gathering embeddings from the main memory.

**Access-aware memory layout for embeddings.** To offer *Hotline*, we leverage the insight that real-world recommender models train on inputs that exhibit *extremely* high popularity skew [7, 8, 12, 44, 48]. This causes certain embedding entries to be accessed several orders-of-magnitude more frequently than others. We refer to these embeddings as *frequently-accessed entries*. The frequently-accessed entries have a small memory footprint while being computationally significant. Keeping this access property in mind, *Hotline* foremost offers an optimized *access-aware memory layout for embeddings* that is utilized by a novel *runtime scheduler to perform mini-batch scheduling onto GPUs to ensure the parameter gathering of embeddings is pipelined with compute*. Our framework stores the frequently-accessed embeddings on GPUs to mitigate their transfer overheads.

**Layout-aware runtime scheduling.** To utilize this memory placement, *Hotline* requires a runtime scheduler that can tackle the challenge that a minibatch of inputs (2K-32K) can access a combination of frequently-accessed and not-frequently-accessed embeddings. While frequently-accessed embeddings are on GPU, accessing the not-frequently-accessed embeddings from main memory can stall the pipeline. The runtime scheduler mitigates this by reforming a small set of mini-batches into two classes. The first class only accesses frequently-accessed embeddings and are directly scheduled onto GPUs. This is because the local GPU memory contains the required working parameters. The second class contains the remaining inputs that access not-frequently-accessed embeddings. To hide the data transfer latency, the scheduler gathers the required working parameters from the CPU memory while the frequently-accessed inputs are being executed on GPUs. The second task needs to be performed in a high-throughput manner to ensure that GPU is not starving during the non-popular inputs. The scheduler overcomes this by offering a novel runtime *accelerator* that sits between the GPUs and the main memory. Thus the accelerator schedules the input mini-batches in a data and model-aware manner and by efficiently gathering embedding parameters from both the GPU (frequently-accessed) and CPU-based main (not-frequently-accessed) memory.

**Contributions:** We make the following contributions:

1. Identify the frequently-accessed embeddings *dynamically* at runtime with negligible overhead.

2. Offer a dynamic data and model-aware scheduler to efficiently pipeline the mini-batch dispatch onto GPUs while concurrently obtaining not-frequently-accessed embeddings from the CPU-based main memory.
3. Offer a runtime framework that increases the training throughput by stitching the recommender model execution onto GPUs – *without* impacting fidelity.

We evaluate *Hotline* with publicly available deep learning (DLRM) and time-sequence (TBSM) based recommendation models. We compare against two baselines. Namely, a hybrid CPU-GPU baseline where CPUs store and compute on embeddings and a GPU-only embedding processing baseline. In both these cases, multiple GPUs parallelize the neural network computations,

For the CPU-GPU hybrid baseline, we compare *Hotline* against state-of-the-art deep learning framework XDL [27] and Intel [30] optimized DLRM. On average, the *Hotline* acceleration pipeline provides  $3.75\times$  speedup over the 4-GPU XDL and  $3\times$  speedup over Intel optimized DLRM while maintaining the baseline accuracy. *Hotline* is able to perform training of larger models such as Terabyte even while using a single GPU, whereas GPU-only baseline requires at least 4 GPUs to store its embeddings. On average, *Hotline* obtains  $1.8\times$  performance benefits over the GPU-only baseline, as it eliminates data movement between the GPU devices.

## 2. Background and Challenges

### 2.1. A Primer on Recommendation Systems

**1. Machine Learning Model:** Recommender models use categorical features and continuous features. Typically, large embedding tables store the categorical features for each user and item. On the other hand, the continuous features are processed by reasonably-sized neural network layers which range from Multi-layer Perceptrons (MLP) to DNNs. Recommendation models are currently among the largest ML models that are being executed in data centers. A recently released recommendation model by Meta contains 12 Trillion parameters [37] in comparison to GPT-3 with 175 Billion parameters [10].

**2. Training Setup:** Large recommender models can be trained in two distributed modes. First, the embeddings are stored and gathered on CPU and the neural networks are executed on GPUs in a data-parallel fashion. Now, the training throughput is throttled by large data transfer and low bandwidth CPU main memory. Figure 2 shows the training time being spent on these operations in 4 real-world models and datasets. We observe that the communication and embedding-bag operation can be as high as 75% for large datasets such as Criteo Terabyte. This presents an opportunity for acceleration.

Second, we can use as many GPUs as required to store the embeddings fully while enabling data-parallel neural-network execution. However, this mode has low compute utilization, because the number of GPUs scale based on embedding sizes and not with the requirements of the neural network. On the

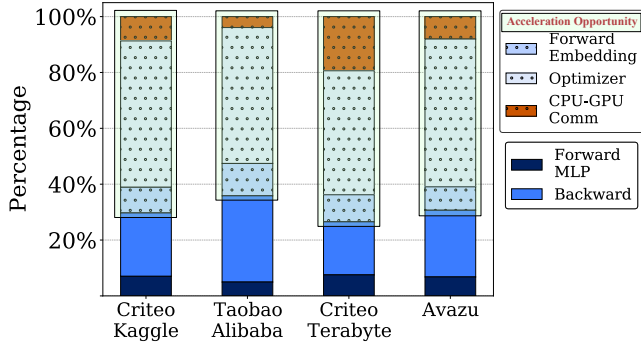


**Figure 2: The breakdown of the training time for an Intel-optimized DLRM with 1 GPU in a hybrid CPU-GPU training setup. The dotted parts of the bar are executed on CPU and present an opportunity for GPU-based acceleration.**

contrary, our paper exploits the semantics of user behaviour, i.e. training input, in recommendation models to efficiently use the memory capacity and improve compute throughput.

**3. Popularity in Training Inputs:** Hotline exploits a key property of recommendation system inputs – that certain users and items observe very high popularity. This implies that some embedding entries are accessed much more frequently. Figure 3 shows that, across real-world datasets, a small number of frequently-accessed embeddings have  $>100\times$  more accesses than others. Our experiments show that simply tracking up to 512 MB of embeddings can help cater to  $>75\%$  of training inputs. Tracking beyond 512 MB of frequently-accessed embeddings only provides diminishing returns. However, exploiting input popularity at a fine granularity is non-trivial.

## 2.2. Challenges in Exploiting Input Popularity

**Limitation – Segregation and Scheduling with CPU:** One could simply employ CPU-based multi-processing to segregate frequently-accessed and not-frequently-accessed embeddings and schedule the corresponding mini-batches. Figure 4 shows that an Intel-Xeon CPU, even after using *all its cores* for multi-processing, has up to  $2.5\times$  higher latency as compared to NVIDIA-V100 GPU(s) executing 4 training iterations. Additionally, as we execute larger mini-batch sizes, the CPU processing overhead and its latency increases proportionately. Therefore, typical CPUs *cannot* complete segregating popular and not-popular mini-batches and schedule them before the GPU(s) finish execution.

**Challenge 1 – Tackle Changing Access Frequency:** Prior works use an *offline* profiler to identify the frequently-accessed embeddings. They use two suppositions [7, 48]. First, that training data is fully available before training. Second, that frequently-accessed embeddings do not change over time.

We observed that training data is typically updated on a daily basis. Thus, one cannot access the full training dataset ahead in time. Furthermore, as the dataset evolves daily and a recent

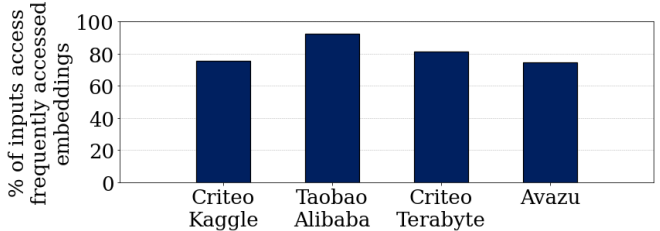
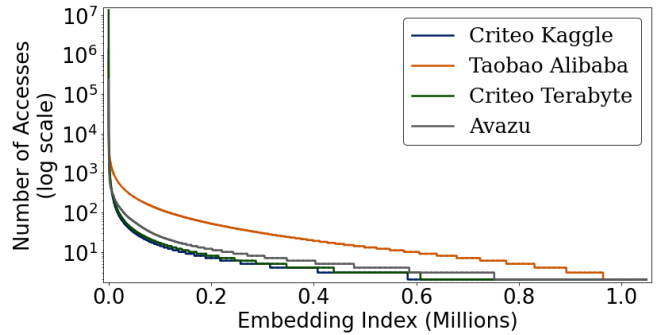


**Figure 3: The frequency of accesses per embedding entry for one training epoch. The frequently-accessed embeddings tend to have more than  $100\times$  more accesses compared to others. Inputs with rate of 1-in-every-100000 embedding accesses are labeled as frequently-accessed.**

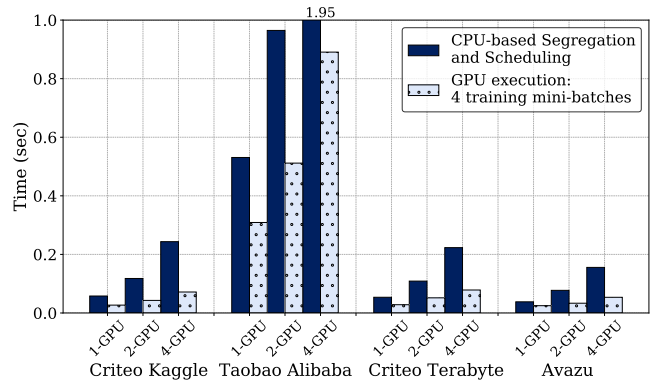


**Figure 4: Comparison of multi-process CPU-based segregation and scheduling time using an Intel Xeon CPU for 4 training iterations with NVIDIA-V100 GPU(s). We use mini-batches of 1K, 2K, and 4K for 1, 2, and 4-GPU execution respectively. Even after using multiprocessing, the CPU has a higher latency and cannot finish segregating and scheduling popular and not-popular mini-batches before the GPU(s) finish execution.**

work, called BigPipe [8], has shown the set of frequently-accessed embeddings also rapidly change over time.

**Challenge 2 – Dynamically Capture the Access Skew:** We need to dynamically determine the frequently-accessed embedding entries at very low latency. This helps avoid extra overheads in the case of online training where training samples could arrive sporadically. We must also adapt to the changing popularity of inputs and update the frequently-accessed

embedding entries continuously with very low overheads.

**Our Approach:** Hotline dynamically determines the frequently-accessed embeddings by processing only a small portion of the training inputs. Hotline uses a novel accelerator to enable fine-grained parallel embedding index tracking across mini-batches. The Hotline accelerator can re-calibrate the frequently-accessed embeddings as the training data changes over time.

**Challenge 3 – Training with Mixed Mini-Batches:** Each mini-batch can require a mix of frequently-accessed and other embeddings. Thus, the working parameters can be spread across the CPU main memory (for not-frequently-accessed embeddings) and GPU’s (for frequently-accessed embeddings) local memory. Consequently, embeddings from the main memory would need to be collected and sent to the GPU before computation. Gathering working parameters using GPUs is not ideal as they are not only inefficient at collecting irregularly scattered embeddings, but would also waste their precious compute cycles on intricate fine-grained operations.

**Our Approach:** The Hotline accelerator uses immensely parallel compute engines that gather several inputs. The accelerator then creates mini-batches of inputs that only access frequently-accessed embeddings and dispatches them to GPUs. While the frequently-accessed inputs are being executed, the accelerator gathers the embeddings from CPU main memory for the remaining not-frequently-accessed embeddings inputs thereby hiding their communication overheads.

### 3. System Design and Execution

The baseline system comprises a server multi-core CPU connected to multiple GPU devices via the PCIe-link. The inter-GPU communication happens through NVLink [3]. Figure 5 shows the Hotline system; it places the accelerator on the *low profile PCIe slot* not being used by a GPU. The accelerator can access the DMA engine via the PCIe switch and can directly communicate with the main memory whilst entirely avoiding the high-overhead CPU pipeline. Hotline does not require any changes to CPU and GPU devices. The accelerator employs two phases during training: (1) The ‘access learning’ phase identifies the frequently-accessed embeddings.(2) The ‘runtime accelerated’ phase pipelines popular and non-popular mini-batches to the GPU.

#### 3.1. Hotline Training Execution Phases

**1. Access Learning Phase** During training runtime, in the first phase, called the access learning phase, the Hotline accelerator samples mini-batches to determine which embeddings are frequently-accessed. This is performed *only* in the

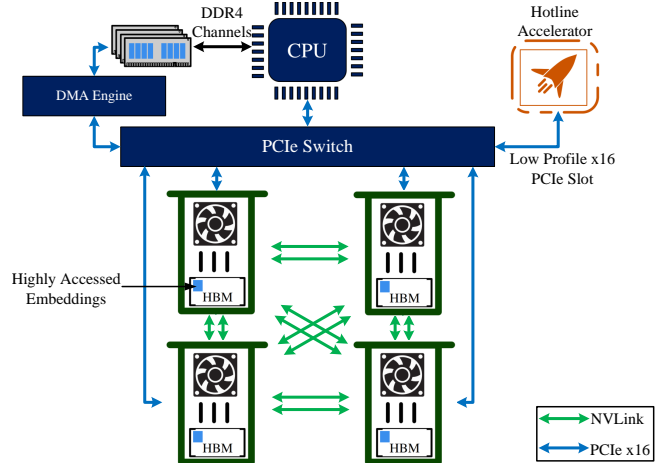


**Figure 5: Hotline’s heterogeneous system architecture. The accelerator sits between the CPU and the GPU(s). It can directly access the main memory to obtain the training inputs and not-frequently-accessed embeddings and relay them to the GPU.**

first epoch *only* for a % of mini-batches. Our experiments show that, the accelerator only needs to sample 5% of the mini-batches for datasets like Criteo Kaggle [14] and Criteo Terabyte [15]. It only needs to sample 15% and 20% of the mini-batches for Avazu [29] and Taobao Alibaba [9] datasets, respectively. Such low-overhead sampling can identify >90% of frequently-accessed embeddings.

During this phase, all the embedding entries are obtained from the CPU main memory and gradually some of these entries are classified as frequently-accessed. Once the first phase completes, the contents of the frequently-accessed embeddings are replicated across all the GPUs. The Hotline accelerator only stores the *indices* of the frequently-accessed embeddings and does not need to store the data contents of frequently-accessed embeddings. The frequently-accessed embedding indices are used by the accelerator to classify popular and non-popular inputs into mini-batches. The detailed execution of the accelerator during this phase is described in Section 4.

**2. Runtime Accelerated Phase** Once the frequently-accessed embeddings are replicated on each GPU, the *runtime accelerated phase* commences. The Hotline accelerator reorders popular and non-popular inputs across a collection of mini-batches. We refer to these mini-batches as the working set of the accelerator. The Hotline accelerator creates *new* mini-batches from this working set.

Now a mini-batch contains inputs that only accesses the frequently-accessed embeddings (popular mini-batch) or contain inputs that access both frequently-accessed and not-frequently-accessed embeddings. As the GPU memories contain the frequently-accessed embeddings, the popular mini-batches can be directly scheduled onto the GPUs. The accelerator obtains the embeddings from both the CPU and GPU memories while GPUs are executing popular minibatches and

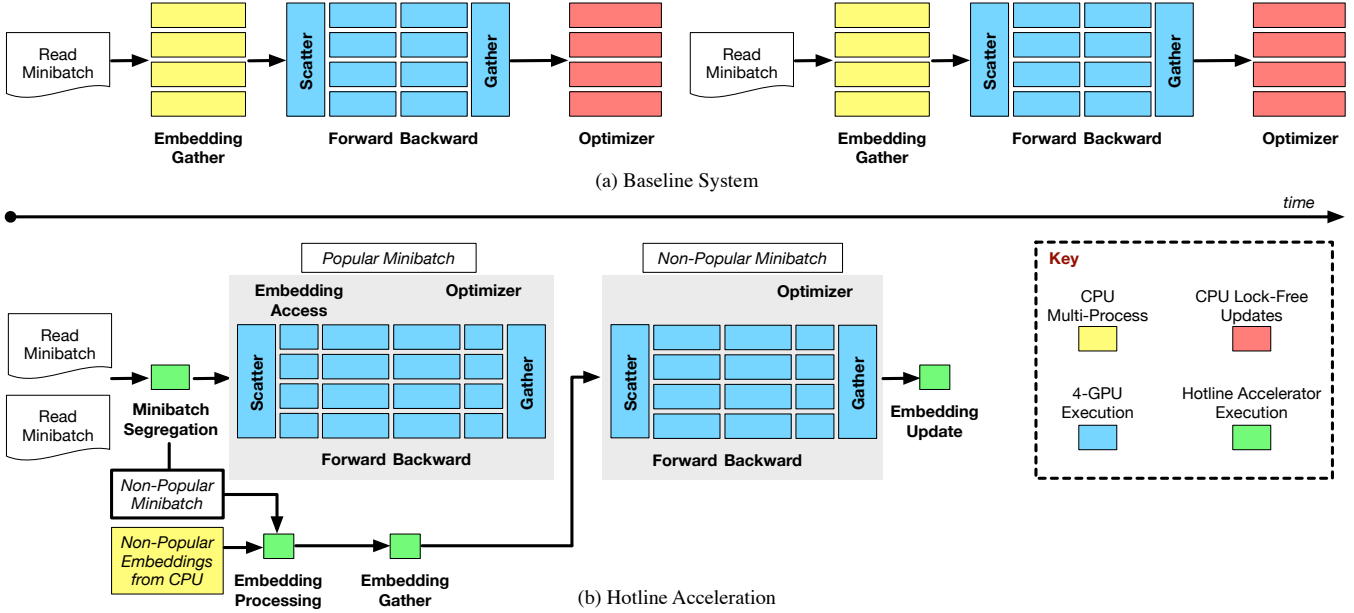


**Figure 6: An example execution pipeline of Hotline training with two mini-batch working set. The accelerator classifies inputs into popular and non-popular mini-batches, schedules the popular one directly on GPU, and in the meantime gathers the working parameters for non-popular one to schedule onto GPU. The accelerator hides the data gather latency behind GPU execution.**

hides the embedding gather latency. CPU and GPU memories have the most updated not-frequently-accessed and frequently-accessed embeddings respectively. Hotline does not encounter any synchronization or cache coherence overheads because the not-frequently-accessed embeddings and frequently-accessed embeddings are always accessed from the CPU main memory and GPUs respectively.

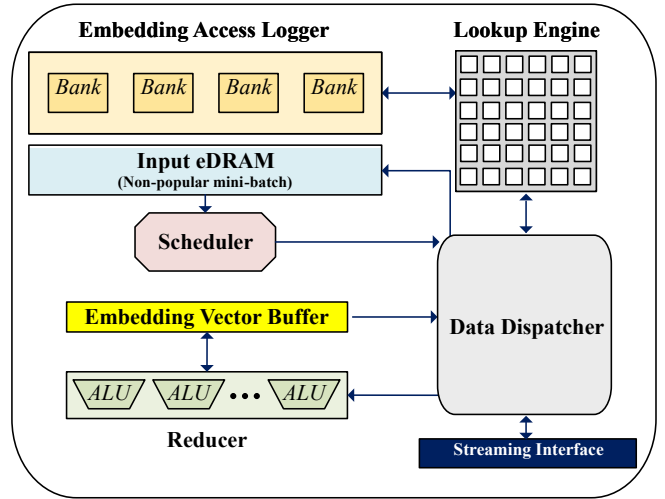
### 3.2. Pipelined Execution at Runtime

Figure 6 shows an example of the pipelined execution across the CPU, the Hotline accelerator, and the GPU. All the training inputs are obtained from the CPU main memory. If we have a working set of four mini-batches, on average, three mini-batches worth of inputs would be popular. This is because, on average,  $>75\%$  of the inputs are popular and they can be directly scheduled onto the GPUs. While the popular mini-batches are executing on the GPU, the accelerator obtains the embeddings for the non-popular minibatch from CPU and GPU memories. Once the GPU is done executing popular mini-batches, the accelerator schedules the non-popular mini-batch to the GPUs along with its working parameters.

The forward and backward pass for the entirety of the recommender model executes on GPUs for both the popular and non-popular mini-batches. This is because, now the required parameters are always in the local GPU memory. As the non-popular mini-batch is executing on the GPU, the accelerator begins to read the next set of mini-batches from the CPU main memory. The details of how the accelerator segregates mini-batches and gathers embeddings are provided in Section 4.4.

## 4. Design: Hotline Accelerator

Figure 7 shows the block diagram of the Hotline accelerator. We describe the micro-architectural details of each component and then provide an example execution flow.



**Figure 7: Block diagram of the Hotline hardware accelerator. The hardware accelerator connects to the low-profile PCIe slot via a Streaming Interface.**

### 4.1. Hotline Accelerator: High-Level Flow

We describe the high-level flow during the access learning and the runtime accelerated phases:

**Access learning phase.** The data dispatcher block reads input mini-batches from CPU main memory via the streaming interface, sends them to the lookup engine block, and updates the embedding access logger (EAL) block. The role of the EAL block is to keep track of the amount of times an embedding index has been accessed across mini-batches. Based on the access pattern of the embedding indices across first few mini-batches, the Hotline accelerator can determine which entries are frequently-accessed. Once this phase completes, all entries in the EAL block becomes read-only.

**Runtime accelerated phase.** The data dispatcher and the scheduler play a vital role. The data dispatcher directs each input in the mini-batch to the lookup engine. The output of the lookup engine then flows into the input classifier. The input classifier marks each incoming input as either popular or non-popular. The non-popular inputs are collected in the *input eDRAM* while the popular inputs are dispatched to the GPU(s). Once a mini-batch worth of non-popular inputs are collected and their working parameters are fetched from GPU and CPU memories, the scheduler dispatches this mini-batch to the GPU devices.

#### 4.2. Hotline Accelerator: Components

**1. Data Dispatcher** Figure 8 shows the block diagram of the the Data Dispatcher block. The *Address Registers* store the base address of each embedding table in the main memory and GPU memory. The *Memory Controller* generates the address using the Address Registers to access the embeddings within the CPU and GPU memories. The *Input Classifier* segregates incoming inputs as popular and non-popular based on availability of embeddings within EAL. While the popular mini-batches are being executed on GPU(s), the dispatcher issues the non-popular mini-batch from the input eDRAM to the Lookup Engine. This enables the Hotline accelerator determine the working parameters of the non-popular mini-batch at runtime.

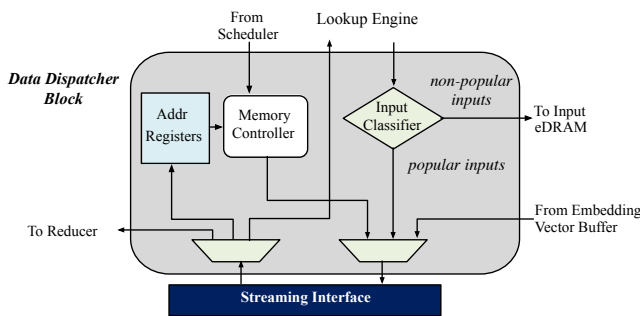


**Figure 8: The Address Registers, Memory Controller, and Input Classifier constitute the Data Dispatcher block.**

A non-popular minibatch consists of inputs that require a mixture of not-frequently-accessed and frequently-accessed embeddings. For accessing the not-frequently-accessed embeddings (present in main memory), the Memory Controller

uses the Address Registers to calculate the embedding address based on the embedding row index and its sparse dimension size. The memory controller then issues a direct memory access (DMA) request to the DMA-engine for not-frequently-accessed embeddings. While for frequently-accessed embeddings, a GPU read memory request is issued. Thereafter, the working parameters obtained from CPU and GPU memory are processed by the Reducer block. This block reduces multiple embedding rows into a single embedding vector and stores it in the *Embedding Vector Buffer*.

**2. Embedding Access Logger (EAL)** During the access learning phase, the *Embedding Access Logger (EAL)* uses counters to track the access frequencies of embedding entries. The logger only stores the indices and not the contents of the embedding entries. As Figure 9 shows EAL consists of a Multi-Banked SRAM, Controller, and an input/output Queue.

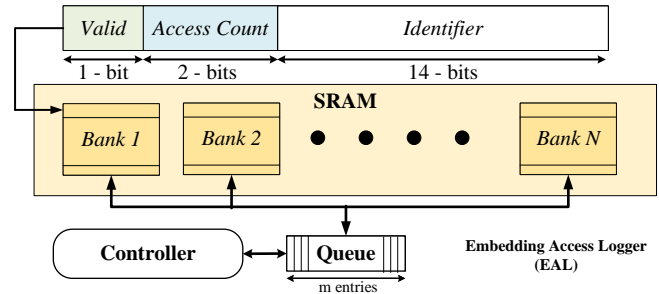


**Figure 9: The block diagram of the components within the Embedding Access Logger (EAL). It consists of an Multi-Banked SRAM, Controller, and Queue sub-blocks.**

**Naive Embedding Tracking.** A naive way to track frequency of accesses into each embedding entry is to use a separate counter for each sparse parameter. As number of sparse parameters can be in the range of billions, this method of tracking would require gigabytes of on-chip storage. Alternatively, storing the frequencies in the CPU/GPU memory will incur 3 accesses - one to obtain the embeddings, one to read the frequency, and another to update the frequency.

**Efficient embedding frequency tracking:** EAL is designed to dynamically track only the frequently-accessed embeddings by using their indices. Our design is motivated by two observations. First, compared to the overall embedding size (10-100 GBs), the size of frequently-accessed embeddings is under 512 MB. Second, the access skews for these entries is extremely high ( $> 100\times$  accesses). Thus, EAL is designed as a cache-like structure that keeps track of frequently-accessed embedding indices. For the purpose of this paper we assume a 4-way set associative SRAM cache. Assuming an embedding dimension of 64, with each entry being 4 Bytes, 512 MB worth of frequently-accessed embeddings contains 2 million indices. Thus, the Hotline accelerator uses a 4 MB SRAM cache with 2 million blocks. As we need to classify embeddings based on their access frequency, we could use the Least Frequently

Used (LFU) replacement policy. However, this would require significant area overheads, as each of these 2 million cache blocks would require 24-bit counters (Figure 3 shows embeddings can have up to 10 million accesses).

To minimize area overheads, EAL uses the static Re-reference Interval Predictor (SRRIP) replacement policy with a 2-bit Re-reference Predictor Value (RRPV) counter [25]. As frequently-accessed embeddings have  $>100\times$  more frequent accesses, a 2-bit RRPV counter with insertions at RRPV-1 value captures  $>99\%$  of the frequently-accessed embeddings. Figure 10 compares SRRIP based optimal logger to an Oracle which has infinite-sized access counters for each embedding entry.

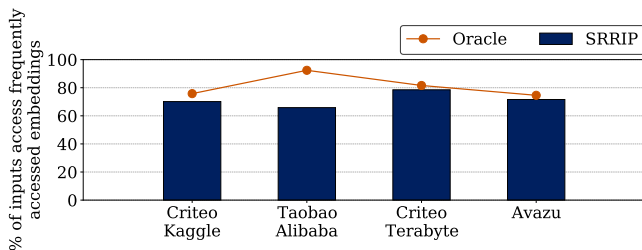


**Figure 10: SRRIP-based tracker as compared to the Oracle LFU scheme. On average, the SRRIP-based tracker can track 70% of the frequently-accessed embeddings.**

The SRRIP based EAL SRAM cache has 70% tracking capability. Note that, even if a non-frequently-accessed embedding is mis-classified as frequently-accessed or vice versa, model correctness does not change.

**Multi-Banked SRAM for multi-embedding lookup.** Each input accesses multiple embeddings within each embedding table. Hotline enables these parallel lookups by dividing EAL into multiple banks. Figure 11 shows our empirical design space exploration wherein the average number of requests issued as the number of banks ( $n$ ) increase while varying input queue size ( $m$ ). On average, a 512-sized queue with 64-banks enables 60 parallel requests into unique banks per iteration. The EAL uses a controller to schedule the incoming requests from lookup engine block to the 512-entry queue.

Once the frequently-accessed embeddings are determined, the EAL switches to stops updating and provides these embedding indices during the runtime accelerated phase. EAL periodically switches back to the access learning phase and captures the changes in popularity,

**3. Lookup Engine** Lookup engine is a parallel 2D compute network that processes on every training input and extracts their embedding entries. For instance, if an input requires 26 distinct embedding tables, the accelerator can achieve 26x throughput per input. Furthermore, the 2D compute network enables exploiting parallelism across training inputs within the mini-batch working set. The Lookup engine, during the access learning phase, provides EAL with the indices accessed by each input for its updates. During the runtime acceler-

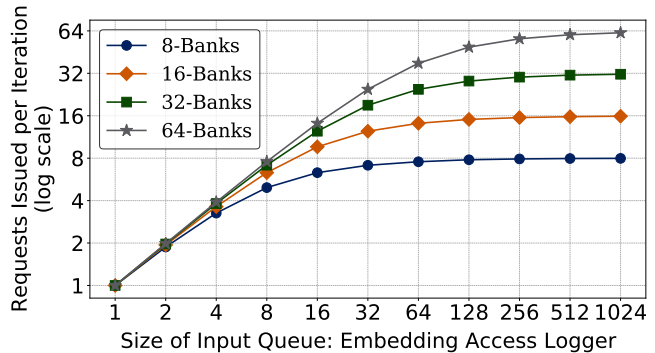


**Figure 11: Impact of Queue Size and Banks on # of parallel requests per iteration. Embedding Access Logger uses a 512 queue with 64-banks to enable 60 parallel requests.**

ated phase, the Lookup Engine tags inputs as popular if all embedding indices are in EAL as frequently-accessed.

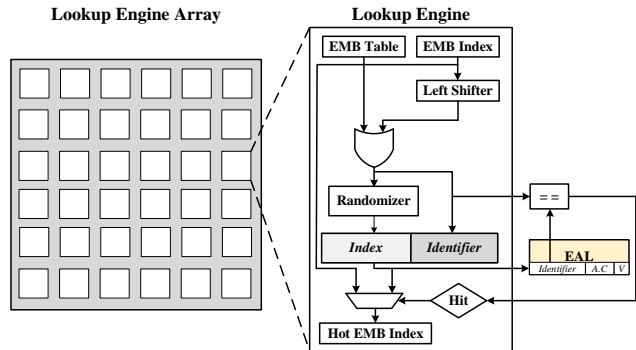


**Figure 12: Architecture of the Lookup Engine. The Lookup engine array determines the embedding entries that are used by a training input.**

Figure 12 shows the components within a single lookup engine. Each engine consists of registers containing embedding table number, embedding index, hot embedding index register and a randomizer. The embedding table number and index for the input are merged and sent to the randomizer. The randomizer creates a hash of the (Embedding Index, Embedding Table) tuple. This hash scatters embedding index values across EAL to avoid trashing during the access learning phase. We implement our randomizer block using a low-latency Fiestal Network implementation [35].

**4. Reducer** The Reducer performs sparse length sum element-wise operation using an array of simple arithmetic units. It reduces multiple embedding rows a table into a single vector (embedding pooling operation) and stores the result in embedding vector buffer.

#### 4.3. Hotline Accelerator: Instruction Set Architecture

As the Hotline accelerator interacts with both the main memory and GPU via the PCIe link, it requires a brief set of instructions (Table 1) to read/write the required data into these

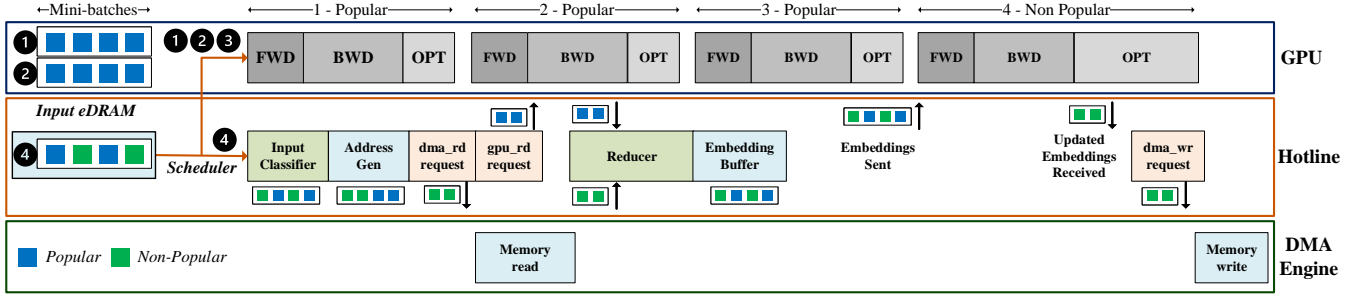


Figure 13: Dataflow through the Hotline accelerator. The accelerator is responsible for re-arranging popular/non-popular inputs, gathering their embeddings, and scheduling them on the GPU.

devices. The Hotline ISA facilitates communication with the DMA engine and GPUs.

Table 1: Hotline Instructions Set

Instruction	Operand 1	Operand 2	Description
<code>dma_rd(op1, op2)</code>	mem start idx	# bytes	DMA read request
<code>dma_wr(op1, op2)</code>	mem start idx	# bytes	DMA write request
<code>v_add(op1, op2)</code>	input vector	emb vec buff	element wise addition
<code>v_mul(op1, op2)</code>	input vector	emb vec buff	element wise dot product
<code>s_wr(op1, op2)</code>	reg idx	base addr	write emb base addr
<code>gpu_rd(op1, op2)</code>	gpu device id	sparse idx	read emb idx from GPU device

#### 4.4. Hotline Accelerator: Tying it together

Figure 13 shows an example execution of the accelerator during the runtime accelerated phase. The Hotline accelerator reads mini-batches from the main memory and segregates them into popular and non-popular sets. In this example we show a working set of 4. Input eDRAM just stores the non-popular mini-batch while popular mini-batches are sent to the GPU(s). The *Scheduler* block organizes the timeline to issue non-popular mini-batch after the popular mini-batches complete execution. Popular mini-batches execute in a data parallel fashion as all the model parameters are present in the local memory of each GPU. Simultaneously, the scheduler sends the inputs of the non-popular mini-batch from *input eDRAM* to the *Lookup Engine* block. The *Lookup Engine* block checks whether the indices are located in the EAL, if so, they are classified as frequently-accessed and obtained from the GPU(s), else are obtained from the main memory.

Each embedding entry obtained from main or GPU memory goes through the *Reducer* block. For multiple embedding lookups within an embedding table, the *Reducer* block applies embedding pooling operation to convert all the lookups into a single embedding vector. Thereafter, the embedding vector is temporarily stored in the *embedding vector buffer*. Once the all the working parameters of non-popular mini-batch have been fetched, the non-popular mini-batch is dispatched along with the embedding vectors. The entire execution including the forward, backward pass, and the optimizer execute on the GPU for all the mini-batches. Once the embedding updates are generated by the optimizer, the updated not-popular embeddings

are stored are written to the CPU main memory. Thus, the CPU maintains the most up-to-date non-frequently-accessed embeddings whereas the GPU stores the frequently-accessed embeddings for the entirety of the training process.

## 5. Evaluation Methodology

### 5.1. Recommender Models

Table 2 illustrates the specifications of four well-established recommender models used to evaluate Hotline. The number of sparse parameters varies from 5.1M (RM1) to 266M (RM3). The number of dense parameters is around 5 orders of magnitude less than the number of sparse parameters. The bottom MLP computes on dense inputs, whereas the top MLP generates the final recommendation for the user. RM1 is a neural network dominated model with top and bottom MLP layers and a deep learning attention layer. RM2 and RM3 models, instead, are embedding dominated as they consist of more sparse features and bigger embedding tables. RM4 has an average size of dense neural network and sparse embedding tables. We use open source implementation of Deep Learning (DLRM) [40] and Time-based Sequence Models (TBSM) [23] benchmarks to train the above mentioned models. TBSM trains the RM1 model and DLRM is used to train RM2, RM3 and RM4 models. TBSM consists of an embedding layer implemented using DLRM and a time-series layer resembles an attention mechanism and contains its own neural networks.

### 5.2. Datasets

We use four real-world datasets to train the above mentioned models. Table 2 shows the details of each dataset. Taobao Alibaba [9] is a user behaviors dataset from Taobao, for recommendation problem with implicit feedback offered by Alibaba. Criteo Kaggle [14] dataset is obtained from Display Advertising Challenge and contains advertising data from Criteo to capture user’s preference by predicting click-through-rate. Criteo Terabyte [15] is the largest publicly available dataset for users click logs. Avazu [29] dataset is taken from click-through-rate prediction competition by Kaggle.

**Table 2: Recommender Model Architecture and Parameters**

Model	Dataset	Time Series	Features		Parameters			Neural Network Configuration			Size (GB)
			Dense	Sparse	Dense	Sparse	Sparse Dim	Bottom MLP	Top MLP	DNN	
RM1	Taobao Alibaba [9]	21	1	3	7.3 k	5.1 M	16	1-16	30-60-1	Attn. Layer	0.3
RM2	Criteo Kaggle [14]	1	13	26	287.5 k	33.8 M	16	13-512-256-64-16	512-256-1	-	2
RM3	Criteo Terabyte [15]	1	13	26	549.1 k	266 M	64	13-512-256-64	512-512-256-1	-	63
RM4	Avazu [29]	1	1	21	281.4 k	9.3 M	16	1-512-256-64-16	512-256-1	-	0.55

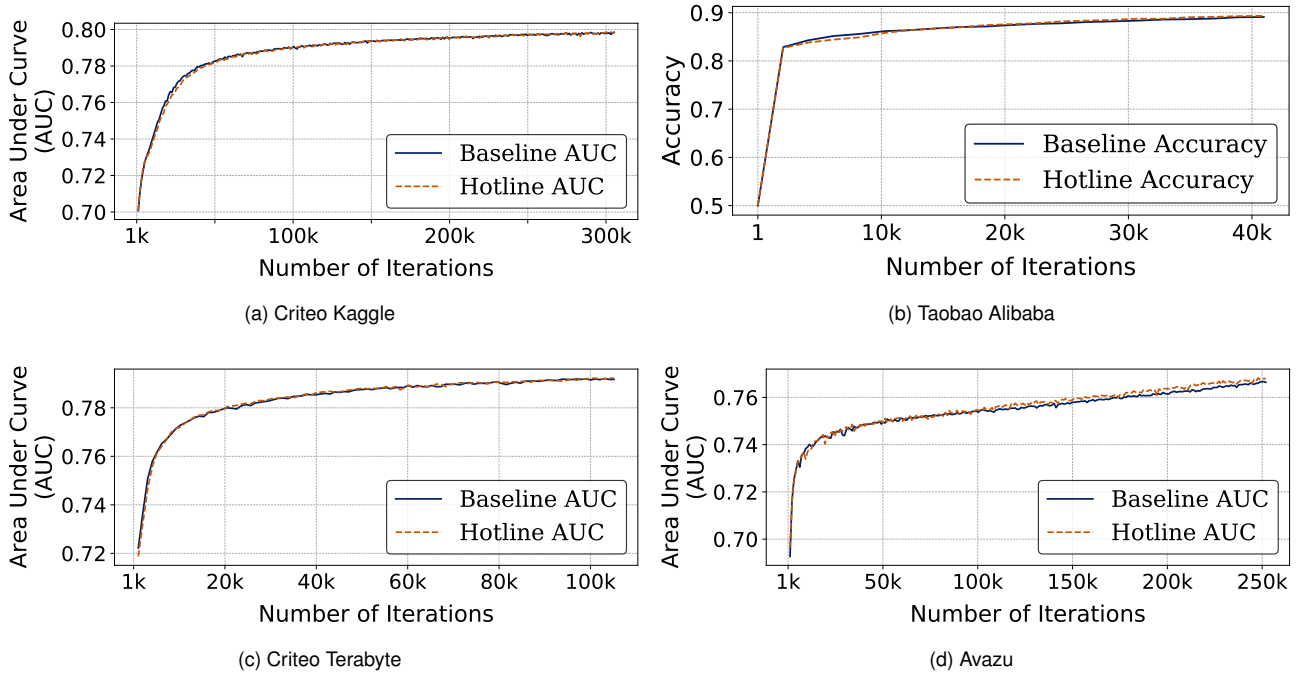


**Figure 14: AUC comparison of Hotline with a baseline system while performing full-precision training. Hotline maintains the training fidelity throughout execution.**

### 5.3. Software libraries and setup

DLRM and TBSM are configured using Pytorch-1.9 using Python-3. We use the *torch.distributed* backend to support scalable distributed training and performance optimization [46]. For all the backend GPU-to-GPU communication such as gather, scatter, and all-reduce collective calls, we use the fast NVIDIA Collective Communication Library (NCCL) [41] on NVLink-2.0. We compare against DLRM and TBSM implementation on XDL [27], Intel-optimized DLRM [30] and FAE [7]. We use Tensorflow-1.2 [5] as computation backend for XDL-based implementation.

### 5.4. Server Architecture

Table 3 shows the details of the server. They comprise 24-core Intel Xeon Silver 4116 (2.1 GHz) processor with Skylake architecture. Each server is connected to 4 NVIDIA Tesla-V100 GPUs. Every GPU and the Hotline accelerator communicates with the rest of the system via a 16x PCIe Gen3 bus. We perform experiments on a single server.

**Table 3: System Specifications**

Device	Architecture	Memory	Storage
CPU	Intel Xeon	192 GB	1.9 TB
	Silver 4116 (2.1 GHz)	DDR4 (2.7 GB/s)	NVMe SSD
GPU	Nvidia Tesla	16 GB	-
	V100 (1.2 GHz)	HBM-2.0 (900 GB/s)	

### 5.5. Runtime measurements.

For the CPU and GPU executions we measure the wall clock time to train the entire model based on its convergence criterion. For Hotline accelerator, we synthesize the architecture implemented in Verilog RTL using Synopsys DC with 45nm technology and validated 350 MHz as the frequency. We obtain the access time of the memory components in the accelerator using Cacti [38]. We used a RTL-simulation for compute cycles and access cycles from Synopsys DC and Cacti to calculate the accelerator runtime. Real system DMA latency and HBM latency are being used for estimating working parameters gathering time. Also we empirically observed that fetching frequently-accessed embeddings alternatively from each GPU device would rule out the GPU HBM contention

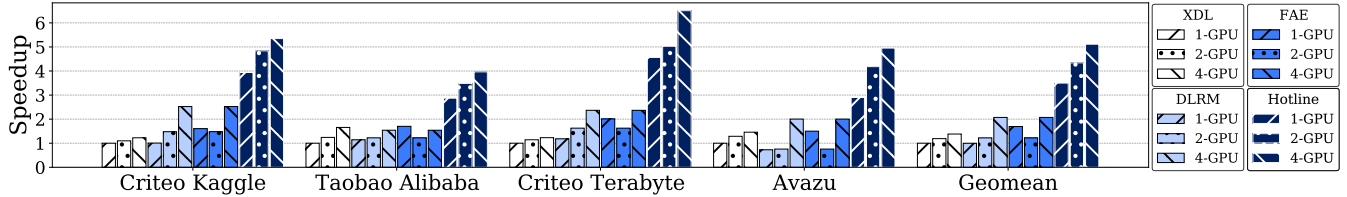


**Figure 15: The performance comparisons Hotline with XDL, Intel optimized DLRM, and FAE implementations (normalized to a 1-GPU XDL). On average, even a 1-GPU Hotline provides 3.5 $\times$  higher performance as compared to the baseline.**

and results in balanced memory load on each GPU device. The details of the accelerator are provided in Table 4. We observe that a size of 2.5 MB for the input eDRAM is sufficient to store 16 K input non-popular mini-batch. The 0.5 KB embedding vector buffer can store an embedding vector with a dimension of 128. We chose the eDRAM [52] technology because of its high storage density. We use a 4 MB embedding access logger (EAL).

**Table 4: Accelerator Specifications**

Parameters	Settings	Parameters	Settings
Frequency	350 MHz	EAL size	4 MB
No of Reducer ALU Units	16	No of Lookup Engines	64
Input eDRAM size	2.5 MB	Embedding Vector Buffer	0.5 kB
Total Area	7.01 mm <sup>2</sup>	Average Energy	132 mJ

## 5.6. Area/Energy measurements of Hotline

We use Cacti [38] to estimate the area/energy of memory components (40 nm technology). We implemented the Verilog RTL and synthesized with Synopsys Design Compiler (45 nm FreePDK process) for other components.

## 6. Results and Analysis

### 6.1. Training Accuracy

Hotline segregates the mini-batches into popular and non-popular ones within the working set. Hence, we evaluate the accuracy implications of Hotline. Figure 14 illustrates the Area Under Curve (AUC) accuracy metric for Criteo Kaggle, Criteo Terabyte, and Avazu datasets as established by MLPerf [1, 53]. For the Taobao dataset, we use the test accuracy – as AUC metric is not offered for the TBSM model. We use full-precision DLRM and TBSM model implementations using Intel’s optimized DLRM [30] for accuracy comparisons. We observe that Hotline completely follows the baseline test and train accuracy. Table 5 compares the testing accuracy, AUC, and cross-entropy loss for all workloads.

### 6.2. End-to-End Performance

#### 1. Performance benefits over hybrid CPU-GPU Baselines

Figure 15 demonstrates the end-to-end training benefits obtained due to Hotline in comparison to three state of the art software implementations with varying number of GPUs. First, XDL [27] is an Industrial Deep Learning Framework that uses a parameter server approach. Here the GPU improves the

**Table 5: Accuracy Metric Comparisons**

Dataset	DLRM			Hotline		
	Accuracy (%)	AUC	Logloss	Accuracy (%)	AUC	Logloss
Criteo Kaggle	78.64	0.798	0.456	78.64	0.798	0.456
Taobao Alibaba	89.11	-	0.270	89.34	-	0.264
Criteo Terabyte	81.20	0.792	0.421	81.21	0.792	0.421
Avazu	83.61	0.766	0.387	83.61	0.768	0.386

efficiency of Advanced Model Server by using a faster embedding dictionary lookup on GPU while CPU is used as backend workers. Second, an Intel-Optimized DLRM [30] implementation, where the embeddings are executed on CPU using lock free updates and neural networks on GPUs in data parallel fashion. Third, a software framework called FAE [7], that uses input popularity but combines *offline pre-processing* with *CPU based scheduling without pipelining*. For the data-parallel approach, we deploy the weak scaling technique where we scale the mini-batch size with number of GPUs, i.e., 1K for 1-GPU setup, 2K for 2-GPU setup, and 4K for 4-GPU. All the numbers are normalized to XDL 1-GPU setup.

As shown in Figure 15, Hotline across all the models, datasets, and settings, reduces the overall training time as it performs the entire recommender model compute on the GPU(s). On average Hotline obtains a speedup of 3.5 $\times$  and 3.5 $\times$  for 1-GPU, 3.15 $\times$  and 3.11 $\times$  for 2-GPU, 3.75 $\times$  and 3 $\times$  for 4-GPU over XDL and optimized DLRM implementations. As compared to a recent contemporary work called FAE [7], Hotline obtains a speedup of 2.3 $\times$ , 2.9 $\times$ , and 3.4 $\times$  for the 1-GPU, 2-GPU, and 4-GPU implementations respectively.

### 6.3. Latency Breakdown

Figure 16 shows the latency breakdown of the two hybrid baselines and Hotline. Hotline incurs a negligible overhead due to its efficient pipelining. For the Criteo Kaggle and Terabyte datasets, which are more embedding and memory intensive, Hotline significantly reduces the CPU-GPU communication time. For the Taobao dataset, which is neural network centric, the deep learning execution overshadows the communication time. Broadly, Hotline always reduces the total compute time.

### 6.4. Comparison Studies

We compare Hotline against a GPU-only Model-Parallel and a CPU-based Hotline implementation.

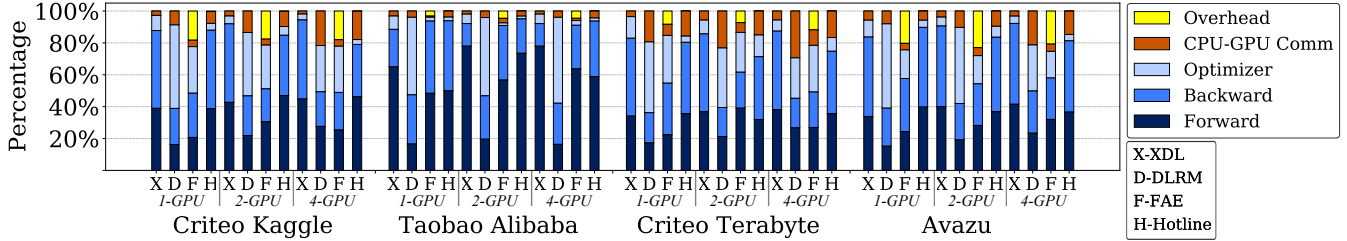


Figure 16: Latency breakdown of 1, 2, and 4 GPU implementations of software frameworks and Hotline. The overhead of CPU-GPU communication time increases as number of GPUs scale because of inter-GPU communication. Note that, unlike Hotline, FAE incurs a reasonably high overhead from embedding synchronization.

**1. GPU-only Model-Parallel Baseline:** We use HugeCTR [2] by Nvidia as the GPU-only baseline. HugeCTR scales the number of GPUs to fit the entire model within GPUs’ local memories and performs model parallel training for embeddings while using data parallel training for the neural network portion. As shown in Figure 17, we compare the performance of Hotline with HugeCTR for two models, Criteo Kaggle and Criteo Terabyte – the only ones offered by the current HugeCTR evaluation. We observe that for a small model like Criteo Kaggle, HugeCTR is able to fit and train the model on a single GPU. The Criteo Kaggle results are thus normalized to 1-GPU HugeCTR. For a large model like Criteo Terabyte, HugeCTR is unable to fit the model within 1 or 2 GPUs; throws an Out of Memory (OOM) error, and requires a minimum of 4 GPUs. Hence, Criteo Terabyte results are normalized to 4-GPUs.

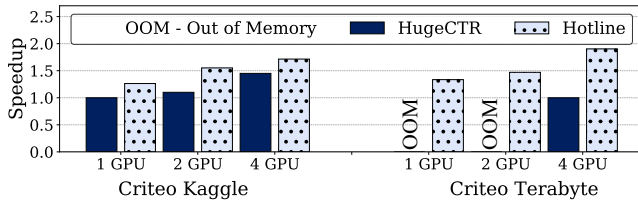


Figure 17: The speedup of Hotline normalized to HugeCTR. Hotline provides a speedup of up to 1.8 $\times$ .

As shown in Figure 17, Hotline removes all-to-all communication associated with model parallel embedding layer of HugeCTR and outperforms in all the cases. Moreover, for popular minibatches Hotline completely execute embeddings and neural layers in data parallel fashion, which mitigates any CPU-GPU communication overheads. For non-popular mini-batches it incurs an overhead of obtaining embeddings from CPU memory. However, this latency is hidden behind the execution of popular mini-batches.

**2. Comparison over CPU-based Hotline:** CPU can be used as an alternative to the Hotline hardware accelerator for re-ordering mini-batches, gathering working set parameters, and as a pipeline scheduler. To enable this, we map the Hotline computation (forward, backward and optimizer) to high throughput GPUs and try to provide working parameters to these GPUs at a rate faster than GPU execution – to avoid

stalls. We observe that mini-batch re-ordering and working parameter gathering are memory intensive operations. This results in data stalls within the CPU it acts as bottleneck.

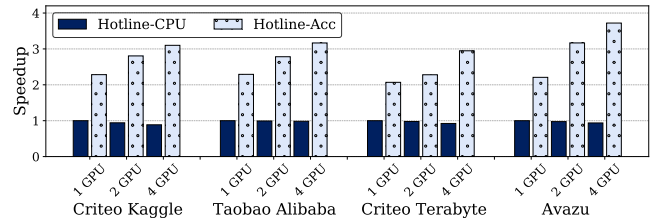


Figure 18: Hotline speedup normalized to CPU-based Hotline implementation. The Hotline hardware accelerator provides up to 3.5 $\times$  speedup as compared to a CPU-based implementation.

Figure 18 shows the performance benefits of Hotline accelerator over a CPU that implements the features of Hotline using multi-processing. As the mini-batch and number of GPUs scale, performance of CPU-based Hotline degrades because of increased data stalls.

## 6.5. Throughput Improvements

Hotline improves the end-to-end training throughput by processing a pipeline of mini-batches. As Figure 19 shows, for a 4-GPU system Hotline can process, on average, 4 $\times$  more epochs/hour as compared to optimized DLRM baseline. Hotline throughput improves at a higher rate with increasing mini-batch than the baseline, because with a larger mini-batch, Hotline can create bigger popular mini-batches.

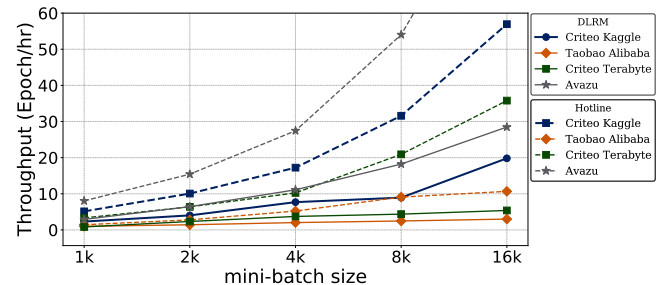


Figure 19: Varying throughput with 4-GPU executions.

### 6.6. CPU to GPU embedding transfer latency

Table 6 shows the absolute time spent by baseline and Hotline to perform CPU to GPU embedding transfers. Hotline reduces the transfer time, on average (4-GPU), by  $2.7\times$ , as popular inputs do not need embeddings from CPU memory.

**Table 6: CPU-GPU data transfer time - 10 Epochs (mins)**

Dataset	1-GPU		2-GPU		4-GPU	
	DLRM	Hotline	DLRM	Hotline	DLRM	Hotline
Criteo Kaggle	17.04	3.16	17.91	3.30	16.89	5.66
Taobao Alibaba	15.65	4.81	15.21	3.30	11.71	3.10
Criteo Terabyte	62.47	12.44	54.27	10.77	47.27	9.21
Avazu	11.96	1.84	14.71	2.13	11.51	2.79

### 6.7. Performance improvement for synthetic models

To understand the efficacy of Hotline as the size recommendation models increase, we generated synthetic models and datasets. Figure 20 shows the performance of Hotline across two synthetic models. Hotline continues to provide up to  $2.5\times$  speedup even as model sizes scale.

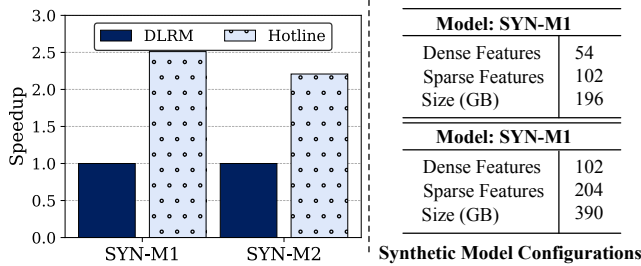


**Figure 20: Performance of Hotline versus Intel-Optimized DLRM across synthetic models for a 1-GPU system.**

### 6.8. Design Space Exploration

**Varying the number of inputs in a mini-batch:** Figure 21 shows the performance benefits of Hotline are accentuated with larger mini-batch sizes. This is due to two reasons, scheduler has to issue input dispatch commands fewer times. Secondly, larger mini-batches offer more parallelism opportunities, and Hotline enables more compute on GPU(s).

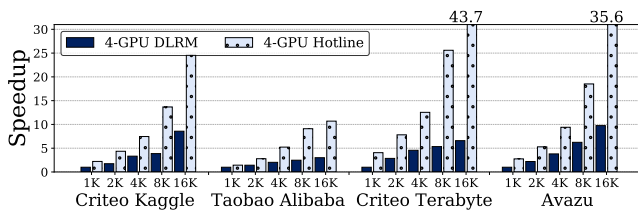


**Figure 21: Hotline speedup with varying mini-batch sizes.**

**Mini-batch working set:** Figure 22 compares the impact of the mini-batch working set on the execution time. For a small

working set, e.g. 1, even if there is a single input which accesses not-frequently-accessed embeddings, the accelerator will have to gather the working parameters for the whole mini-batch. This data transfer latency cannot be hidden behind the popular input execution and causes a bottleneck. We observe that a 4 mini-batch working set is sufficient to completely fill the pipeline and extract maximum throughput.

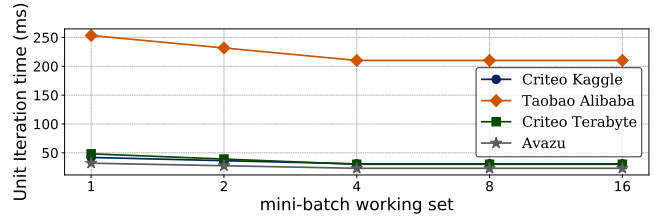


**Figure 22: Effect of varying working set on unit iteration time.**

**Embedding Access logger size:** Figure 23 shows the percentage of inputs accessing frequently-accessed embeddings captured by varying the logger size. For Criteo and Avazu datasets with more skewness, even a small 2MB logger can capture most of the frequently-accessed indices. However for Taobao dataset, that has a lower skew, once the logger size is increased beyond 4 MB we observe diminishing returns.

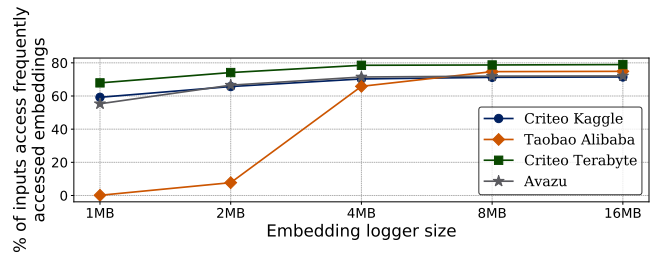


**Figure 23: Percentage of inputs accessing frequently accessed embeddings captured with varying logger size.**

**Table 7: Area and Power Breakdown**

Component	Area	Power
EAL	65.72%	67.31%
Input eDRAM	23.44%	26.75%
Lookup Engine	5.80%	2.97%
Emb Vec Buffer	0.66%	0.99%
Others	4.38%	1.98%

**Hotline Accelerator Area and Power Breakdown.** Table 7 shows the area and power division across different components of Hotline accelerator. Embedding access logger consumes the most area and power as it is a 4-way set associative structure with replacement policy logic. The next significant area consuming component is Input eDRAM as this memory structure is used to store non-popular inputs. Finally, the lookup engine

consumes the least percentage of area and power as it only performs lookup logic.

## 7. Related Work

Industry-scale recommender datasets show that accesses depict a Power or Zipfian distribution [7, 56].

**Recommendation models and designs:** In this work we focus on deep learning based recommender models as they are commonly used in production and consume large number of compute cycles in data centres [19, 39]. Even with their popularity, much of the research has focused on optimizing the inference phase of these models [19, 20, 22, 33, 42]. Unlike inference, training is throughput optimized and tends to be more compute and memory intensive. Certain solutions that offer training optimizations [18, 50] or acceleration [31, 36, 45] do not maximize throughput by facilitating better memory and bandwidth utilization of a distributed GPU system.

**Embedding parameter placement:** Work in [6, 57] offers different embedding table placements either through hierarchical parameter server or on different devices, however, treat all embedding entries equally, without the concept of frequently-accessed embeddings and do not deal with perceptive input pre-processing to reduce the overhead of communication between devices. Work in [16] propose techniques to store embedding tables in non-volatile memories and allocate a certain portion of DRAM for caching. Recent work in [18, 31, 37, 50] has also proposed solutions to accelerate near-memory processing for embedding tables. All of these works do not facilitate distributed training of entire recommender models using GPUs. Hotline, instead offers an entirely runtime solution to efficiently pipeline embedding gather and store operations from external memory.

**Optimizations to mitigate memory intensive training:** Prior work [43], optimizes training by modifying the model either through mixed-precision [55] training or eliminating rare categorical variables to reduce the embedding table size. Such approaches that change the data representation and/or embedding tables, require accuracy re-validation across a variety of models and datasets. More work has been done on compression [24, 51, 54] and sparsity [17] to reduce the memory footprint of machine learning models in general. Hotline, on the other hand, performs full-precision training without employing overheads such as compression/decompression and sparse operations by leveraging the skewed access patterns for embeddings. Hotline is orthogonal to these techniques and can be used with them to improve the memory efficiency.

**Machine learning accelerators:** There has been a plethora of work on designing accelerators to execute compute portion of deep learning models [11, 13, 28, 32, 34, 36, 45, 47, 49]. Certain works have also offered accelerators for recommender models, especially collaborative filtering based models [36, 45]. Hotline does not aim to design a specialized architecture to optimize the compute of deep learning based recommender

models. Hotline facilitates training by efficiently dispatching and gathering working parameters and input mini-batches to an already established GPU based system. Nevertheless, Hotline accelerator can be used to enhance the overall benefits of deep learning accelerators by pipelining their execution efficiently.

## 8. Conclusions

Production-scale recommendation models deploy DNNs along with capacity and bandwidth-constrained embedding tables. In this paper, we present Hotline, a heterogeneous acceleration pipeline based on the insight that small portion of embedding tables are frequently accessed. Hotline aims to dispatch popular inputs that only access these frequently-accessed embeddings directly to GPU, while obtaining the not-frequently-accessed embedding data for non-popular inputs. To perform the dynamic segregation and dispatching, we offer a novel accelerator that can perform the fine grained tasks of determining which inputs require what embedding entries, and if needed gather them from main memory and dispatch the inputs. As such, Hotline hides the data transfer latency of obtaining non-frequently-accessed embedding data behind GPU execution of popular inputs. Results on real-world datasets and recommender models show that Hotline reduces the average training time by  $3\times$  and  $1.8\times$  in comparison to Intel optimized CPU-GPU DLRM and HugeCTR optimized GPU-only baseline, respectively.

## Acknowledgements

This project is part of the *STAR Lab* at the University of British Columbia (UBC). We express our thanks to the entire team of the Advanced Research Computing center at UBC [4]. This work was partially supported by the Natural Sciences and Engineering Research Council of Canada (NSERC) [funding reference number RGPIN-2019-05059]. The views and conclusions contained herein are those of the authors and should not be interpreted as necessarily representing the official policies or endorsements, either expressed or implied, of NSERC, the Canadian Government, Microsoft, or UBC.

## References

- [1] MLPerf Benchmarks. <https://mlcommons.org/en/training-normal-10/>.
- [2] NVIDIA Merlin: HugeCTR. <https://github.com/NVIDIA-Merlin/HugeCTR>.
- [3] NVlink.
- [4] UBC Advanced Research Computing, "UBC ARC Sockeye." UBC Advanced Research Computing, 2019, doi: 10.14288/SOCKEYE.
- [5] Martín Abadi, Ashish Agarwal, Paul Barham, Eugene Brevdo, Zhifeng Chen, Craig Citro, Greg Corrado, Andy Davis, Jeffrey Dean, Matthieu Devin, Sanjay Ghemawat,

- Ian Goodfellow, Andrew Harp, Geoffrey Irving, Michael Isard, Yangqing Jia, Rafal Jozefowicz, Lukasz Kaiser, Manjunath Kudlur, Josh Levenberg, Dan Mané, Rajat Monga, Sherry Moore, Derek Murray, Chris Olah, Mike Schuster, Jonathon Shlens, Benoit Steiner, Ilya Sutskever, Kunal Talwar, Paul Tucker, Vincent Vanhoucke, Vijay Vasudevan, Fernanda Viégas, Oriol Vinyals, Pete Warden, Martin Wattenberg, Martin Wicke, Yuan Yu, and Xiaoqiang Zheng. TensorFlow: Large-Scale Machine Learning on Heterogeneous Distributed Systems, 2015.
- [6] Bilge Acun, Matthew Murphy, Xiaodong Wang, Jade Nie, Carole-Jean Wu, and Kim Hazelwood. Understanding Training Efficiency of Deep Learning Recommendation Models at Scale, 2020.
- [7] Muhammad Adnan, Yassaman Ebrahimzadeh Maboud, Divya Mahajan, and Prashant Nair. Accelerating Recommendation System Training by Leveraging Popular Choices. In *VLDB*, 2022.
- [8] Saurabh Agarwal, Ziyi Zhang, and Shivaram Venkataraman. Bagpipe: Accelerating deep recommendation model training, 2022.
- [9] Alibaba. User Behavior Data from Taobao for Recommendation. <https://tianchi.aliyun.com/dataset/dataDetail?dataId=649&userId=1>.
- [10] Tom B. Brown, Benjamin Mann, Nick Ryder, Melanie Subbiah, Jared Kaplan, Prafulla Dhariwal, Arvind Neelakantan, Pranav Shyam, Girish Sastry, Amanda Askell, Sandhini Agarwal, Ariel Herbert-Voss, Gretchen Krueger, Tom Henighan, Rewon Child, Aditya Ramesh, Daniel M. Ziegler, Jeffrey Wu, Clemens Winter, Christopher Hesse, Mark Chen, Eric Sigler, Mateusz Litwin, Scott Gray, Benjamin Chess, Jack Clark, Christopher Berner, Sam McCandlish, Alec Radford, Ilya Sutskever, and Dario Amodei. Language models are few-shot learners, 2020.
- [11] Yu-Hsin Chen, Joel Emer, and Vivienne Sze. Eyeriss: A Spatial Architecture for Energy-Efficient Dataflow for Convolutional Neural Networks. In *ISCA*, 2016.
- [12] K. Cho, M. Lee, K. Park, T. T. Kwon, Y. Choi, and Sangheon Pack. WAVE: Popularity-based and collaborative in-network caching for content-oriented networks. In *2012 Proceedings IEEE INFOCOM Workshops*, pages 316–321, 2012.
- [13] Eric Chung, Jeremy Fowers, Kalin Ovtcharov, , Adrian Caulfield, Todd Massengill, Ming Liu, Mahdi Ghandi, Daniel Lo, Steve Reinhardt, Shlomi Alkalay, Hari Angepat, Derek Chiou, Alessandro Forin, Doug Burger, Lisa Woods, Gabriel Weisz, Michael Haselman, and Dan Zhang. Serving DNNs in Real Time at Datacenter Scale with Project Brainwave. *IEEE Micro*, 38:8–20, March 2018.
- [14] CriteoLabs. Criteo Display Ad Challenge. <https://www.kaggle.com/c/criteo-display-ad-challenge>.
- [15] CriteoLabs. Terabyte Click Logs. <https://labs.criteo.com/2013/12/download-terabyte-click-logs>.
- [16] Assaf Eisenman, Maxim Naumov, Darryl Gardner, Misha Smelyanskiy, Sergey Pupyrev, Kim Hazelwood, Asaf Cidon, and Sachin Katti. Bandana: Using non-volatile memory for storing deep learning models. *Proceedings of Machine Learning and Systems*, 1:40–52, 2019.
- [17] Jeremy Fowers, Kalin Ovtcharov, Karin Strauss, Eric Chung, and Greg Stitt. A High Memory Bandwidth FPGA Accelerator for Sparse Matrix-Vector Multiplication. In *International Symposium on Field-Programmable Custom Computing Machines*. IEEE, May.
- [18] A. Ginart, M. Naumov, D. Mudigere, Jiyan Yang, and J. Zou. Mixed Dimension Embeddings with Application to Memory-Efficient Recommendation Systems. *ArXiv*, abs/1909.11810, 2019.
- [19] U. Gupta, C. Wu, X. Wang, M. Naumov, B. Reagen, D. Brooks, B. Cottel, K. Hazelwood, M. Hempstead, B. Jia, H. S. Lee, A. Malevich, D. Mudigere, M. Smelyanskiy, L. Xiong, and X. Zhang. The Architectural Implications of Facebook’s DNN-Based Personalized Recommendation. In *2020 IEEE International Symposium on High Performance Computer Architecture (HPCA)*, pages 488–501, 2020.
- [20] Udit Gupta, Samuel Hsia, Vikram Saraph, Xiaodong Wang, Brandon Reagen, Gu-Yeon Wei, Hsien-Hsin S Lee, David Brooks, and Carole-Jean Wu. DeepRecSys: A System for Optimizing End-To-End At-scale Neural Recommendation Inference. *arXiv preprint arXiv:2001.02772*, 2020.
- [21] Jui-Ting Huang, Ashish Sharma, Shuying Sun, Li Xia, David Zhang, Philip Pronin, Janani Padmanabhan, Giuseppe Ottaviano, and Linjun Yang. *Embedding-Based Retrieval in Facebook Search*, page 2553–2561. Association for Computing Machinery, New York, NY, USA, 2020.
- [22] Rangi Hwang, Taehun Kim, Youngeun Kwon, and Minsoo Rhu. Centaur: A Chiptlet-based, Hybrid Sparse-Dense Accelerator for Personalized Recommendations. *arXiv preprint arXiv:2005.05968*, 2020.

- [23] T. Ishkhanov, M. Naumov, X. Chen, Y. Zhu, Y. Zhong, A. G. Azzolini, C. Sun, F. Jiang, A. Malevich, and L. Xiong. Time-based Sequence Model for Personalization and Recommendation Systems. *CoRR*, abs/2008.11922, 2020.
- [24] A. Jain, A. Phanishayee, J. Mars, L. Tang, and G. Pekhimenko. Gist: Efficient Data Encoding for Deep Neural Network Training. In *2018 ACM/IEEE 45th Annual International Symposium on Computer Architecture (ISCA)*, pages 776–789, 2018.
- [25] Aamer Jaleel, Kevin B. Theobald, Simon C. Steely, and Joel Emer. High Performance Cache Replacement Using Re-Reference Interval Prediction (RRIP). In *Proceedings of the 37th Annual International Symposium on Computer Architecture*, ISCA '10, page 60–71, New York, NY, USA, 2010. Association for Computing Machinery.
- [26] Myeongjae Jeon, Shivaram Venkataraman, Amar Phanishayee, unjie Qian, Wencong Xiao, and Fan Yang. Analysis of Large-Scale Multi-Tenant GPU Clusters for DNN Training Workloads. In *Proceedings of the 2019 USENIX Conference on Usenix Annual Technical Conference*, USENIX ATC '19, page 947–960, USA, 2019. USENIX Association.
- [27] Biye Jiang, Chao Deng, Huimin Yi, Zelin Hu, Guorui Zhou, Yang Zheng, Sui Huang, Xinyang Guo, Dongyue Wang, Yue Song, Liqin Zhao, Zhi Wang, Peng Sun, Yu Zhang, Di Zhang, Jinhui Li, Jian Xu, Xiaoqiang Zhu, and Kun Gai. XDL: An Industrial Deep Learning Framework for High-Dimensional Sparse Data. *DLP-KDD '19*, New York, NY, USA, 2019. Association for Computing Machinery.
- [28] Norman P. Jouppi, Cliff Young, Nishant Patil, David Patterson, Gaurav Agrawal, Raminder Bajwa, Sarah Bates, Suresh Bhatia, Nan Boden, Al Borchers, Rick Boyle, Pierre-luc Cantin, Clifford Chao, Chris Clark, Jeremy Coriell, Mike Daley, Matt Dau, Jeffrey Dean, Ben Gelb, Tara Vazir Ghaemmaghami, Rajendra Gotipati, William Gulland, Robert Hagmann, C. Richard Ho, Doug Hogberg, John Hu, Robert Hundt, Dan Hurt, Julian Ibarz, Aaron Jaffey, Alek Jaworski, Alexander Kaplan, Harshit Khaitan, Daniel Killebrew, Andy Koch, Naveen Kumar, Steve Lacy, James Laudon, James Law, Diemthu Le, Chris Leary, Zhuyuan Liu, Kyle Lucke, Alan Lundin, Gordon MacKean, Adriana Maggiore, Maire Mahony, Kieran Miller, Rahul Nagarajan, Ravi Narayanaswami, Ray Ni, Kathy Nix, Thomas Norrie, Mark Omernick, Narayana Penukonda, Andy Phelps, Jonathan Ross, Matt Ross, Amir Salek, Emad Samadiani, Chris Severn, Gregory Sizikov, Matthew Snelham, Jed Souter, Dan Steinberg, Andy Swing, Mercedes Tan, Gregory Thorson, Bo Tian, Horia Toma, Erick Tuttle, Vijay Vasudevan, Richard Walter, Walter Wang, Eric Wilcox, and Doe Hyun Yoon. In-Datcenter Performance Analysis of a Tensor Processing Unit. In *Proceedings of the 44th Annual International Symposium on Computer Architecture*, ISCA '17, page 1–12, New York, NY, USA, 2017. Association for Computing Machinery.
- [29] Kaggle. Avazu mobile ads CTR. <https://www.kaggle.com/c/avazu-ctr-prediction>.
- [30] Dhiraj Kalamkar, Evangelos Georganas, Sudarshan Srinivasan, Jianping Chen, Mikhail Shiryaev, and Alexander Heinecke. Optimizing Deep Learning Recommender Systems Training on CPU Cluster Architectures. In *Proceedings of the International Conference for High Performance Computing, Networking, Storage and Analysis*, SC '20. IEEE Press, 2020.
- [31] L. Ke, U. Gupta, B. Y. Cho, D. Brooks, V. Chandra, U. Diril, A. Firoozshahian, K. Hazelwood, B. Jia, H. S. Lee, M. Li, B. Maher, D. Mudigere, M. Naumov, M. Schatz, M. Smelyanskiy, X. Wang, B. Reagen, C. Wu, M. Hempstead, and X. Zhang. RecNMP: Accelerating Personalized Recommendation with Near-Memory Processing. In *2020 ACM/IEEE 47th Annual International Symposium on Computer Architecture (ISCA)*, pages 790–803, 2020.
- [32] Hyoukjun Kwon, Ananda Samajdar, and Tushar Krishna. MAERI: Enabling Flexible Dataflow Mapping over DNN Accelerators via Reconfigurable Interconnects. In *Proceedings of the Twenty-Third International Conference on Architectural Support for Programming Languages and Operating Systems*, ASPLOS '18, page 461–475, New York, NY, USA, 2018. Association for Computing Machinery.
- [33] Youngeun Kwon, Yunjae Lee, and Minsoo Rhu. TensorDimm: A practical near-memory processing architecture for embeddings and tensor operations in deep learning. In *Proceedings of the 52nd Annual IEEE/ACM International Symposium on Microarchitecture*, pages 740–753, 2019.
- [34] Daofu Liu, Tianshi Chen, Shaoli Liu, Jinhong Zhou, Shengyuan Zhou, Olivier Teman, Xiaobing Feng, Xuehai Zhou, and Yunji Chen. PuDianNao: A Polyvalent Machine Learning Accelerator. In *Proceedings of the Twentieth International Conference on Architectural Support for Programming Languages and Operating Systems*, ASPLOS '15, pages 369–381, New York, NY, USA, 2015. ACM.
- [35] Michael Luby and Charles Rackoff. How to construct pseudorandom permutations from pseudorandom functions. *SIAM Journal on Computing*, 17(2):373–386, 1988.

- [36] Divya Mahajan, Jongse Park, Emmanuel Amaro, Hardik Sharma, Amir Yazdanbakhsh, Joon Kim, and Hadi Esmaeilzadeh. TABLA: A unified template-based framework for accelerating statistical machine learning. March 2016.
- [37] Dheevatsa Mudigere, Yuchen Hao, Jianyu Huang, Zhihao Jia, Andrew Tulloch, Srinivas Sridharan, Xing Liu, Mustafa Ozdal, Jade Nie, Jongsoo Park, Liang Luo, Jie Amy Yang, Leon Gao, Dmytro Ivchenko, Aarti Basant, Yuxi Hu, Jiyan Yang, Ehsan K. Ardestani, Xiaodong Wang, Rakesh Komuravelli, Ching-Hsiang Chu, Serhat Yilmaz, Huayu Li, Jiyuan Qian, Zhuobo Feng, Yinbin Ma, Junjie Yang, Ellie Wen, Hong Li, Lin Yang, Chonglin Sun, Whitney Zhao, Dimitry Melts, Krishna Dhulipala, KR Kishore, Tyler Graf, Assaf Eisenman, Kiran Kumar Matam, Adi Gangidi, Guoqiang Jerry Chen, Manoj Krishnan, Avinash Nayak, Krishnakumar Nair, Bharath Muthiah, Mahmoud khorashadi, Pallab Bhattacharya, Petr Lapukhov, Maxim Naumov, Ajit Mathews, Lin Qiao, Mikhail Smelyanskiy, Bill Jia, and Vijay Rao. Software-Hardware Co-design for Fast and Scalable Training of Deep Learning Recommendation Models, 2021.
- [38] Naveen Muralimanohar, Rajeev Balasubramonian, and Norm Jouppi. Optimizing NUCA Organizations and Wiring Alternatives for Large Caches with CACTI 6.0. In *MICRO*, 2007.
- [39] Maxim Naumov, John Kim, Dheevatsa Mudigere, Srinivas Sridharan, Xiaodong Wang, Whitney Zhao, Serhat Yilmaz, Changkyu Kim, Hector Yuen, Mustafa Ozdal, Krishnakumar Nair, Isabel Gao, Bor-Yiing Su, Jiyan Yang, and Mikhail Smelyanskiy. Deep Learning Training in Facebook Data Centers: Design of Scale-up and Scale-out Systems. *arXiv e-prints*, page arXiv:2003.09518, March 2020.
- [40] Maxim Naumov, Dheevatsa Mudigere, Hao-Jun Michael Shi, Jianyu Huang, Narayanan Sundaraman, Jongsoo Park, Xiaodong Wang, Udit Gupta, Carole-Jean Wu, Alisson G. Azzolini, Dmytro Dzhulgakov, Andrey Mallevich, Iliia Cherniavskii, Yinghai Lu, Raghuraman Krishnamoorthi, Ansha Yu, Volodymyr Kondratenko, Stephanie Pereira, Xianjie Chen, Wenlin Chen, Vijay Rao, Bill Jia, Liang Xiong, and Misha Smelyanskiy. Deep Learning Recommendation Model for Personalization and Recommendation Systems. *CoRR*, abs/1906.00091, 2019.
- [41] Nvidia. NVIDIA Collective Communications Library (NCCL). <https://docs.nvidia.com/deeplearning/nccl/index.html>.
- [42] Nvidia. Accelerating wide deep recommender inference on gpus, 2017. <https://developer.nvidia.com/blog/accelerating-wide-deep-recommender-inference-on-gpus/>.
- [43] Mengdi Huang Nvidia Inc. Vinh Nguyen, Tomasz Grel. Optimizing the Deep Learning Recommendation Model on NVIDIA GPUs. <https://developer.nvidia.com/blog/optimizing-dlrm-on-nvidia-gpus>.
- [44] Fragkiskos Papadopoulos, Maksim Kitsak, M. A. Serrano, Marian Boguna, and Dmitri Krioukov. Popularity versus similarity in growing networks. *Nature*, 489(7417):537–40, Sep 27 2012.
- [45] Jongse Park, Hardik Sharma, Divya Mahajan, Joon Kyung Kim, Preston Olds, and Hadi Esmaeilzadeh. Scale-Out Acceleration for Machine Learning. October 2017.
- [46] Adam Paszke, Sam Gross, Soumith Chintala, Gregory Chanan, Edward Yang, Zachary DeVito, Zeming Lin, Alban Desmaison, Luca Antiga, and Adam Lerer. Automatic differentiation in PyTorch. 2017.
- [47] B. Reagen, P. Whatmough, R. Adolf, S. Rama, H. Lee, S. K. Lee, J. M. Hernández-Lobato, G. Wei, and D. Brooks. Minerva: Enabling Low-Power, Highly-Accurate Deep Neural Network Accelerators. In *2016 ACM/IEEE 43rd Annual International Symposium on Computer Architecture (ISCA)*, pages 267–278, June 2016.
- [48] Geet Sethi, Bilge Acun, Niket Agarwal, Christos Kozyrakis, Caroline Trippel, and Carole-Jean Wu. Recshard: Statistical feature-based memory optimization for industry-scale neural recommendation, 2022.
- [49] Hardik Sharma, Jongse Park, Divya Mahajan, Emmanuel Amaro, Joon Kyung Kim, Chenkai Shao, Asit Mishra, and Hadi Esmaeilzadeh. From High-Level Deep Neural Models to FPGAs. October 2016.
- [50] Hao-Jun Michael Shi, Dheevatsa Mudigere, Maxim Naumov, and Jiyan Yang. *Compositional Embeddings Using Complementary Partitions for Memory-Efficient Recommendation Systems*, page 165–175. Association for Computing Machinery, New York, NY, USA, 2020.
- [51] Yang Sun, Fajie Yuan, Min Yang, Guoao Wei, Zhou Zhao, and Duo Liu. A Generic Network Compression Framework for Sequential Recommender Systems. In *Proceedings of the 43rd International ACM SIGIR Conference on Research and Development in Information Retrieval, SIGIR '20*, page 1299–1308, New York, NY, USA, 2020. Association for Computing Machinery.

- [52] G. Wang, D. Anand, N. Butt, A. Cestero, M. Chudzik, J. Ervin, S. Fang, G. Freeman, H. Ho, B. Khan, B. Kim, W. Kong, R. Krishnan, S. Krishnan, O. Kwon, J. Liu, K. McStay, E. Nelson, K. Nummy, P. Parries, J. Sim, R. Takalkar, A. Tessier, R.M. Todi, R. Malik, S. Stiffler, and S.S. Iyer. Scaling deep trench based eDRAM on SOI to 32nm and Beyond. In *2009 IEEE International Electron Devices Meeting (IEDM)*, pages 1–4, 2009.
- [53] Carole-Jean Wu, Robin Burke, Ed H. Chi, Joseph Konstan, Julian McAuley, Yves Raimond, and Hao Zhang. Developing a Recommendation Benchmark for MLPerf Training and Inference, 2020.
- [54] Xiaorui Wu, Hong Xu, Honglin Zhang, Huaming Chen, and Jian Wang. Saec: similarity-aware embedding compression in recommendation systems. In *Proceedings of the 11th ACM SIGOPS Asia-Pacific Workshop on Systems*, pages 82–89, 2020.
- [55] Jie Amy Yang, Jianyu Huang, Jongsoo Park, Ping Tak Peter Tang, and Andrew Tulloch. Mixed-Precision Embedding Using a Cache, 2020.
- [56] Chunxing Yin, Bilge Acun, Xing Liu, and Carole-Jean Wu. TT-Rec: Tensor Train Compression for Deep Learning Recommendation Models, 2021.
- [57] Weijie Zhao, Deping Xie, Ronglai Jia, Yulei Qian, Ruiquan Ding, Mingming Sun, and Ping Li. Distributed Hierarchical GPU Parameter Server for Massive Scale Deep Learning Ads Systems, 2020.